



Time dependent conduction heat transfer during solidification in a storage system using nanoparticles

M. Sheikholeslami¹ · S. A. Shehzad² · Zhixiong Li^{3,4} · Ahmad Shafee⁵ · F. M. Abbasi⁶

Received: 3 July 2018 / Accepted: 6 July 2018 / Published online: 18 July 2018
© Springer-Verlag GmbH Germany, part of Springer Nature 2018

Abstract

In this research, nanofluid thermal behavior in an energy storage system is illustrated by means of FEM. CuO nanoparticles have been dispersed into the water to overcome the poor thermal conductivity. Role of Brownian motion is included for estimating characteristics of nanofluid. Results are shown as solid fraction, isotherm contours, average temperature and total energy profiles. Results showed that dispersing nanoparticles to pure PCM have important impact on heat transfer rate. As A and N enhances, total energy and solidification time decrease. Furthermore, in order to reach greatest solidification rate, nanoparticles with $d_p = 40$ nm should be used.

Abbreviations

NEPCM Nano-enhanced PCM
FEM Finite element method
PCM Phase change material

Subscripts

nf NEPCM
 f Pure PCM
 p Particle

List of symbols

C_p Heat capacity
 L_f Latent heat of fusion
 k Thermal conductivity

Greek symbols

α Thermal diffusivity (m^2/s)
 ρ Fluid density
 ϕ Concentration of NEPCM

1 Introduction

In recent decade, one of the effective heat storage methods in which phase change materials is used, has been attracted various scientists attention. Latent heat thermal energy storage has various uses because PCMs have great heat capacity. The disadvantage of PCMs is low thermal conductivity. This limitation can be solved by adding nanoparticles into pure PCMs (Haq et al. 2017a; Sheikholeslami et al. 2018b; Hayat et al. 2016a; Mushtaq et al. 2014). Chamkha et al. (2010) investigated melting influence on hydrothermal treatment over a vertical plate. They studied non-Newtonian thermal radiation in a permeable media. Sheikholeslami and Rokni (2017) published a report for application of ferrofluid. Comprehensive review paper has been published by Sheikholeslami and Ganji (2016) to show importance of nanotechnology. Haq et al. (2017b) investigated carbon nanotubes pulsatile flow due to magnetic forces in an annulus. Sheikholeslami and Chamkha (2016) depicted the nanofluid treatment in presence of Coulomb force. Hassan et al. (2016) showed the innovative models for predicting solar radiation. Sobamowo (2016) utilized semi analytical method to analyze nanofluid slip boundary conditions.

Hayat et al. (2017) demonstrated slip impact of nanofluid in a rotating system. Tao and He (2015) presented the

✉ S. A. Shehzad
ali_qau70@yahoo.com

¹ Department of Mechanical Engineering, Babol Noshirvani University of Technology, Babol, Iran

² Department of Mathematics, COMSATS University Islamabad, Sahiwal 57000, Pakistan

³ School of Engineering, Ocean University of China, Qingdao 266110, China

⁴ School of Mechanical, Materials, Mechatronic and Biomedical Engineering, University of Wollongong, Wollongong, NSW 2522, Australia

⁵ Public Authority of Applied Education and Training, College of Technological Studies, Applied Science Department, Shuwaikh, Kuwait

⁶ Department of Mathematics, COMSATS University Islamabad, Islamabad 44000, Pakistan

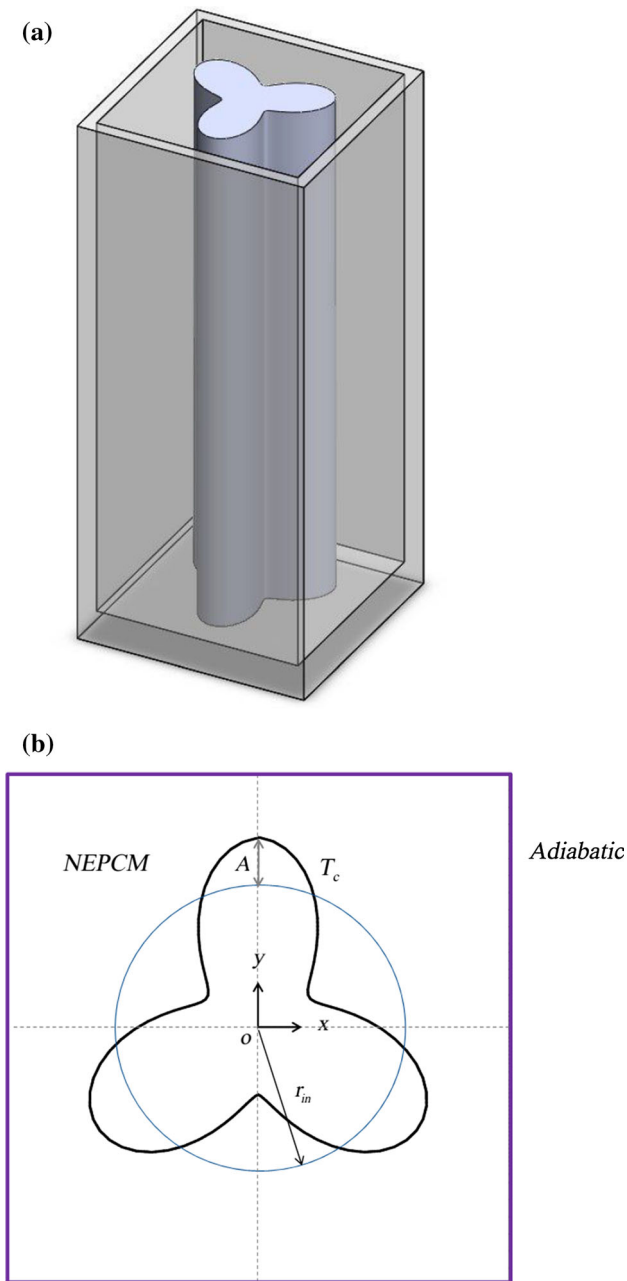


Fig. 1 **a** Three-dimensional view of LHTESS; **b** two dimensional solution domain

Table 1 The physical properties of water as PCM, CuO as nanoparticles and aluminum fin

Property	PCM	Nanoparticles
ρ (kg/m ³)	997	6500
C_p (j/kg K)	4179	540
k (w/mK)	0.6	18
d_p (nm)	–	29
L_f (j/kg)	335,000	–

Table 2 The coefficient values of CuO–water nanofluids

Coefficient values	CuO–water
a_1	– 26.593310846
a_2	– 0.403818333
a_3	– 33.3516805
a_4	– 1.915825591
a_5	6.42185846658E–02
a_6	48.40336955
a_7	– 9.787756683
a_8	190.245610009
a_9	10.9285386565
a_{10}	– 0.72009983664

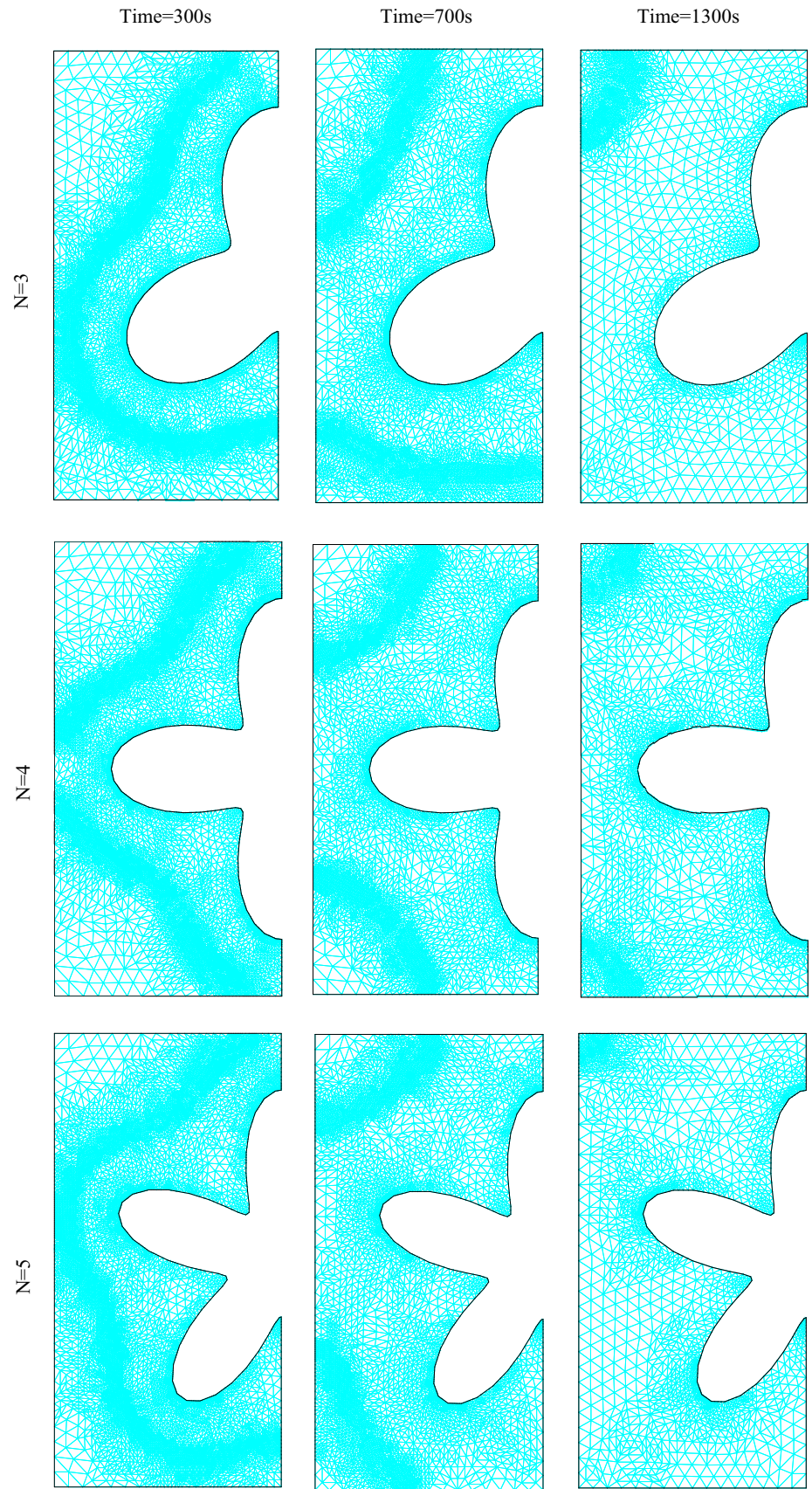
NEPCM charging process in an energy storage system. Ahmed et al. (2017) reported time dependent flow on a heated surface. Ellahi et al. (2016) demonstrated the roles of nanoparticles' size on second law analysis on a wedge. Darzi et al. (2016) simulated the influence of number of fins (4, 10, 15, 20), and volume concentration (0, 2, 4%) of copper nanoparticles as additive on the charging and discharging of PCM. They indicated that dispersing 4% nanoparticles to the water reduce the melting time by 46% while the solidification time reduces just by 16%. Garoosi et al. (2016) employed numerical approach to simulate nanofluid behavior in a heat exchanger with hot pipes. Shahzad et al. (2016) examined Buongiorno model for nanofluid transportation in a sinusoidal duct. Abro and Khan (2017) studied the Casson fluid MHD transportation in a porous media. They did not consider singular kernel in their equations. Selecting effective working fluid becomes hot topics in recent years (Hayat et al. 2016b; Raju et al. 2016; Ahmad and Mustafa 2016; Sheikholeslami and Ellahi 2015; Li et al. 2016; Sheikholeslami et al. 2018a).

In current paper, impacts of utilizing NEPCM on transient heat transfer rate were studied. This transient process was simulated by FEM. Results demonstrate the effects of nanofluid volume fraction, d_p , N and A .

2 Problem explanation

Figure 1a shows the thermal storage shape. The enclosure is filled with NEPCM. Table 1 shows the nanoparticles and pure PCM properties. Complex shape of inner cylinder helps solidification rate. Boundary conditions are shown in Fig. 1b.

Fig. 2 Adaptive mesh refinement procedure when $A = 0.5$, $\phi = 0.04$, $d_p = 30$ nm



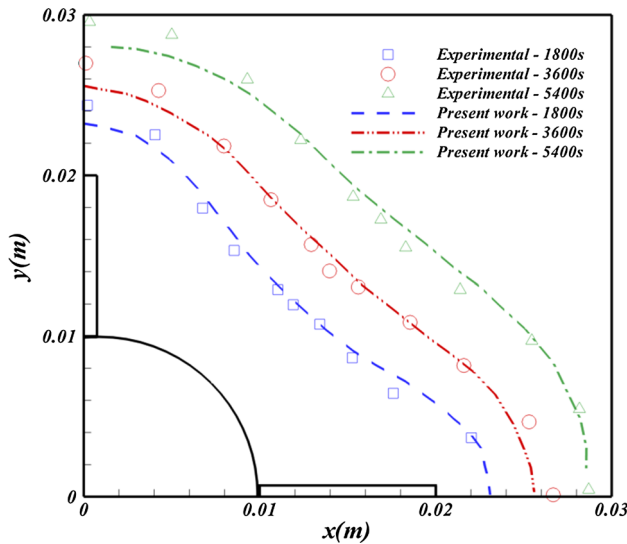


Fig. 3 Comparison between solidification front in fin-assisted LHTESS in present study and experimental work by Ismail et al. (2001)

3 Formulation of problem

Transient heat conduction within solidification can be presented by these formulas:

$$(\rho C_p)_{nf} \frac{dT}{dt} = \nabla(k_{nf} \nabla T) + L_{nf} \frac{dS}{dt} \tag{1}$$

$$\begin{cases} S = 0 & T > (T_m + T_0) \\ S = 1 & T < (-T_0 + T_m) \\ S = (0.5T_0 - T + T_m)/T_0 & (-T_0 + T_m) < T < (T_m + T_0) \end{cases} \tag{2}$$

$(\rho C_p)_{nf}$, ρ_{nf} and $(\rho L)_{nf}$ of NEPCM are:

$$(\rho C_p)_{nf} = \phi(\rho C_p)_p + (\rho C_p)_f(1 - \phi) \tag{3}$$

$$\rho_{nf} = \rho_p \phi + (1 - \phi)\rho_f \tag{4}$$

$$(\rho L)_{nf} = (\rho L)_f(1 - \phi) \tag{5}$$

k_{nf} can be predicted by below formulas (Sheikholeslami 2018):

$$\begin{aligned} R_f &= 4 \times 10^{-8} \text{ km}^2/\text{W}, \quad R_f = -d_p/k_p + d_p/k_{p,eff}, \\ g'(d_p, T, \phi) &= \text{Ln}(T) \left(a_2 \text{Ln}(d_p) + a_5 \text{Ln}(d_p)^2 \right. \\ &\quad \left. + a_1 + a_3 \text{Ln}(\phi) + a_4 \text{Ln}(d_p) \text{Ln}(\phi) \right) \\ &\quad + \left(a_6 + a_8 \text{Ln}(\phi) + a_{10} \text{Ln}(d_p)^2 + a_7 \text{Ln}(d_p) + a_9 \text{Ln}(d_p) \text{Ln}(\phi) \right) \\ \frac{k_{nf}}{k_f} &= 1 + 5 \times 10^4 \rho_f \phi \sqrt{\frac{\kappa_b T}{\rho_p d_p}} c_{p,f} g'(d_p, T, \phi) \\ &\quad - 3 \frac{(1 - k_p/k_f) \phi}{(k_p/k_f + 2) + \phi(1 - k_p/k_f)}. \end{aligned} \tag{6}$$

Table 2 demonstrates the needed constant parameters. E_{total} and T_{ave} should be obtained as:

$$E_{total} = \int (s(\rho L)_{nf} + (\rho C_p)_{nf} T) dV \tag{7}$$

$$T_{ave} = \frac{\int T dA}{\int dA}. \tag{8}$$

4 FEM and validation

Galerkin finite element method with grid refinement was applied to solve this unsteady process. Unsteady terms are estimated by implicit backward difference method. Newton–Raphson method was employed to solve final equations. This code is validated by comparing the result with previous experimental approach. Figures 2 and 3 represent the adaptive mesh and verification, respectively.

5 Results and discussion

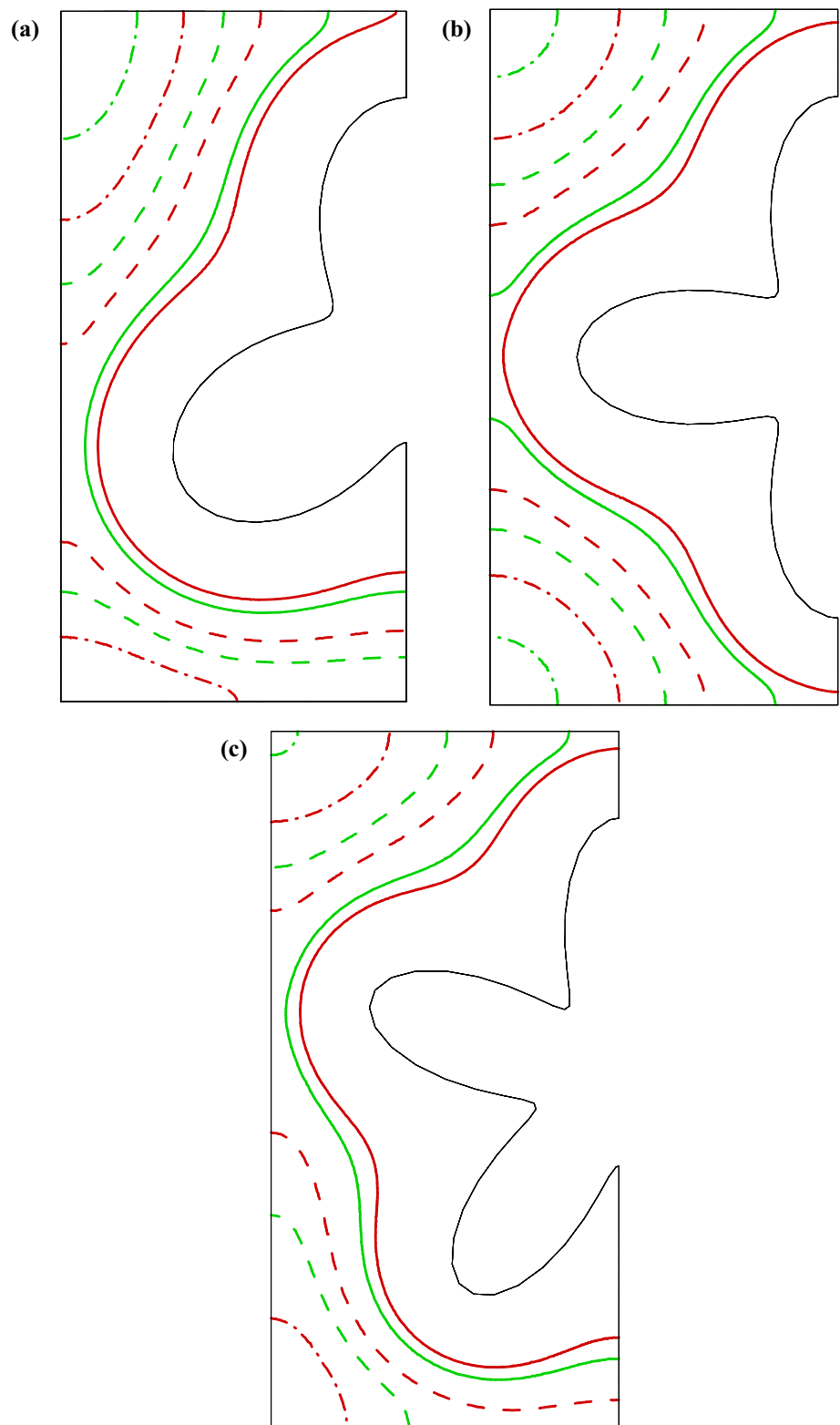
In current research, the effect of using NEPCM on discharging process is simulated by means of FEM. Sinusoidal shape inner cylinder and NEPCM are utilized to accelerate solidification process. Outputs present the effects of nanofluid volume fraction ($\phi = 0-0.04$), size of nanoparticles ($d_p = 30-50 \text{ nm}$), number of undulations ($N = 5, 4, 3$) and amplitude ($A = 0.1, 0.3, 0.5$).

Figure 4 depicts the influence of adding CuO into pure fluid on phase change front. This figure proves that dispersing CuO to pure PCM have important influence on discharging rate. This is because of domination of conduction mechanism in solidification. As shown in this figure, adding CuO nanoparticles helps solidification process. For instance, solidification is done 1.36 times faster than pure PCM when $d_p = 30 \text{ nm}$, $A = 0.5$, $N = 5$. Furthermore, as time progresses the influence of ϕ become more sensible.

Solid fraction and isotherms contours in various time steps are illustrated in Figs. 5, 6 and 7. Just half of geometry can be shown because the geometry is symmetric. As amplitude and number of undulations augments, solidification process takes shorter time. Solidification front progress sooner by using higher A and N . So, this process becomes completed in lower times.

According to obtained data, increasing A , makes this process faster than before. So, it can be concluded that influence of amplitude is more sensible in higher values of N . Similar behavior is obtained for number of undulations. It means that influence of N has higher effect for greater values of A . In $A = 0.5$, $N = 5$, the best performance of

Fig. 4 Effect of adding nanoparticles into PCM on Phase change front [$\phi = 0$, red ($\phi = 0$), green ($\phi = 0.04$)] at various times [time = 300 s (solid line), time = 700 s (broken line), time = 1300 s (dotted broken line)] when $A = 0.5$, $d_p = 30$ nm (color figure online)



LHTESS is obtained and solidification of NEPCM is completed after 1334.3 s. This case depicts the fast solidification process.

Average temperature variations and S_{ave} are demonstrated in the Figs. 8 and 9. Maximum values of average temperature and minimum values of solid fraction obtain at beginning of process. As A and N enhance, the cold wall

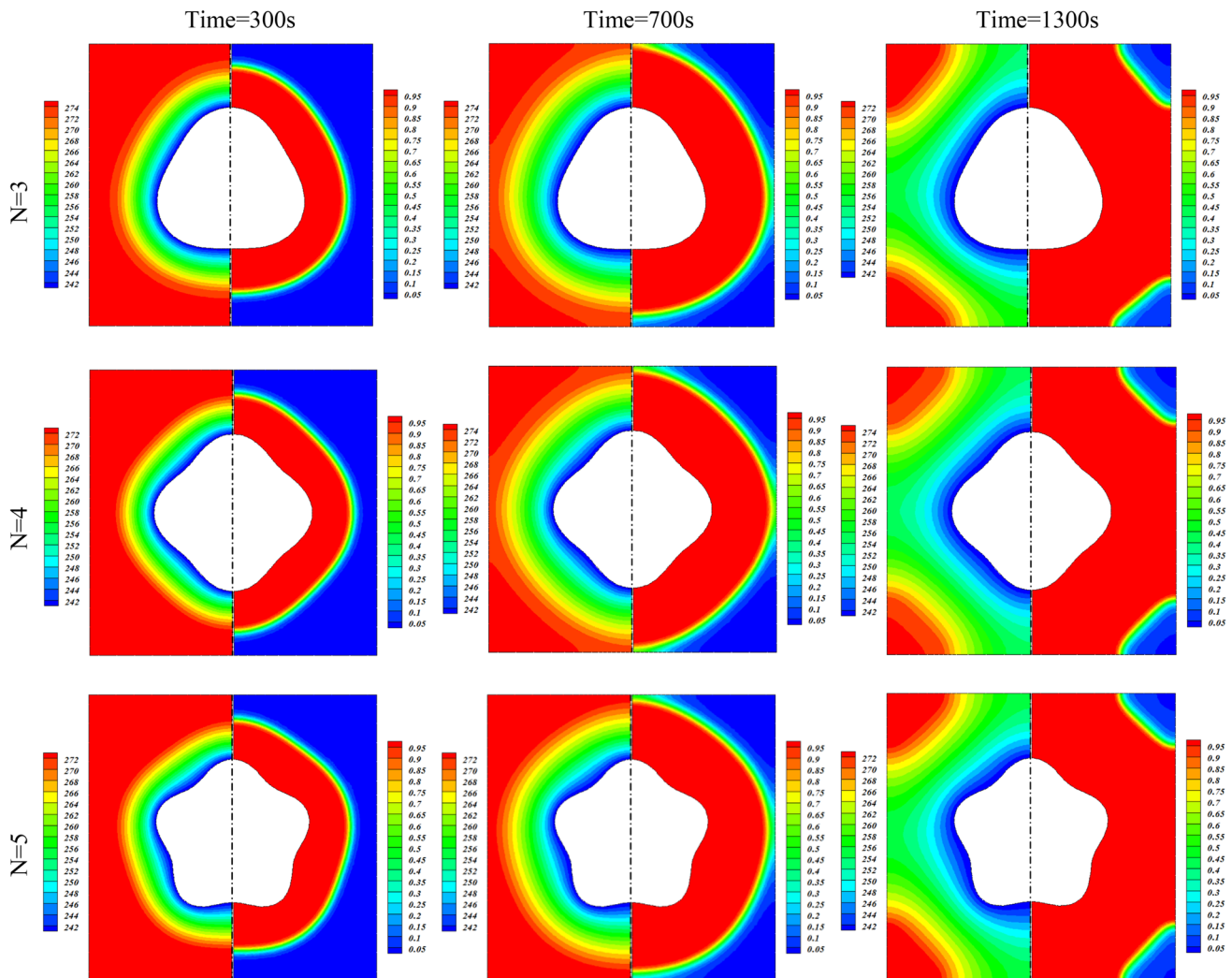


Fig. 5 Solid fraction (right side) and temperature (left side) contour plots at three different time steps during solidification process of LHTESS when $A = 0.1$, $d_p = 30$ nm

has more significant impact on NEPCM. Outputs prove that the lowest full solidification time can be obtained for highest values of ϕ , A , N . This observation is clear from related diagrams and contour.

Figure 10 demonstrates total energy of solidification in LHTESS. This parameter can be calculated as sum of latent and sensible heat. As A and N enhances, total energy decreases. This means that increasing these parameters can improve solidification process. This figure shows that maximum of E_{total} exists at the beginning of solidification.

Effect of d_p on discharging rate is presented in Fig. 11. As demonstrated in this figure, increasing d_p , at first increases the discharging rate but after 40 nm, opposite observation is observed. Effects of d_p , N on S_{ave} , E_{total} and T_{ave} are depicted in the Figs. 12, 13 and 14. Maximum value of S_{ave} and minimum values of T_{ave} are obtained for $d_p = 40$ nm.

Influences of N , d_p , A on full discharging time have been shown in Fig. 15. The related formula is:

$$\begin{aligned}
 Time = & 8021.7 - 224.72 d_p + 52.67 N + 580.58 A \\
 & - 1.67 (N)(d_p) + 0.16(A)(d_p) - 367.73(A)(N) \\
 & + 4.45(d_p^2) + 2.04(N^2) - 327.9(A^2).
 \end{aligned} \tag{9}$$

Using NEPCM instead of PCM makes solidification rate to improve due to augment of thermal properties. As A and N augments, the full solidification time decreases. Penetration depth increases with augment of A and N . So phase change front reach to outer wall in lower time. By using higher values of A , N , the area influenced by cold wall will be broader and heat transfer improves more sensible. Also this figure indicates that $d_p = 40$ nm has the lowest $Time$.

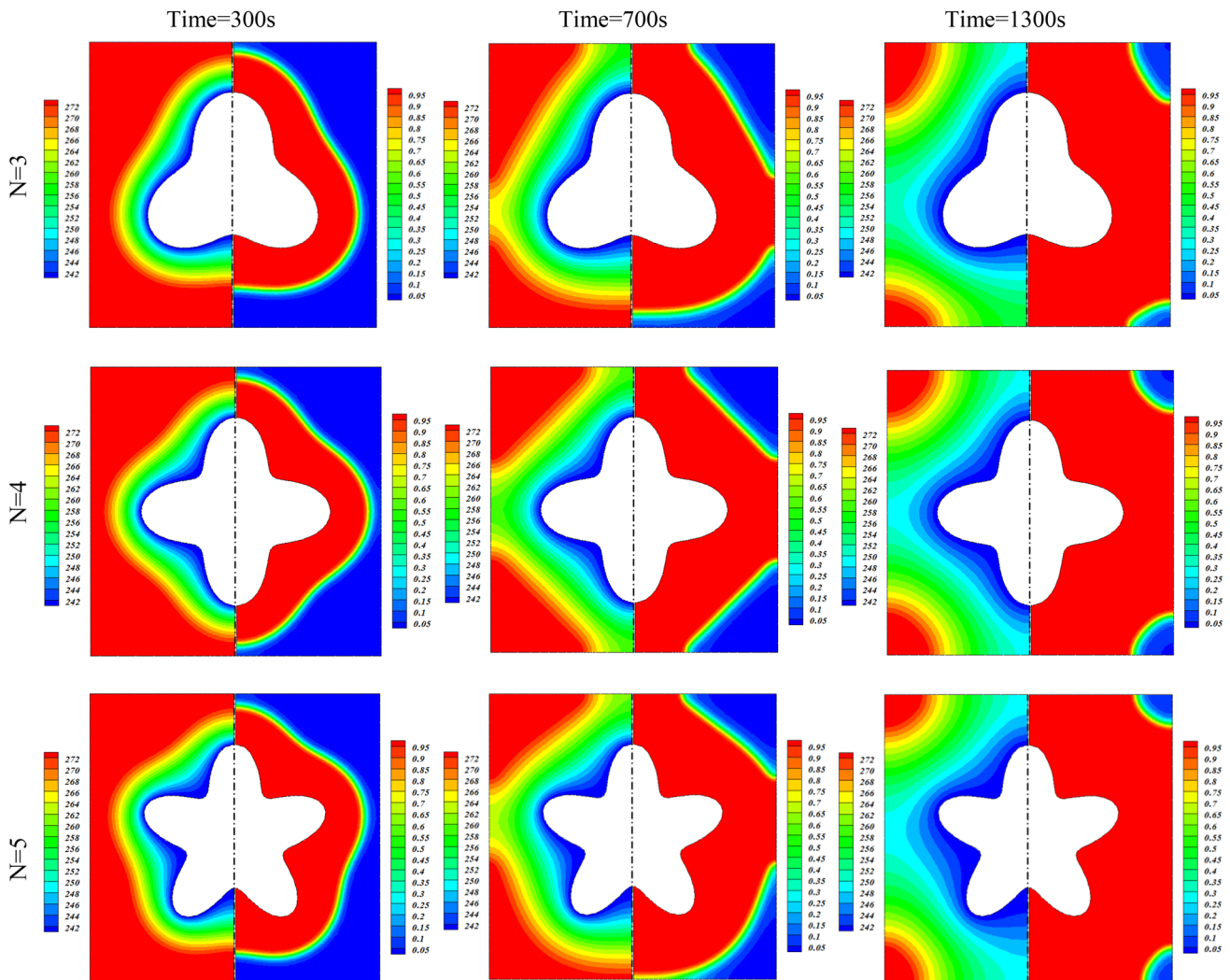


Fig. 6 Solid fraction (right side) and temperature (left side) contour plots at three different time steps during solidification process of LHTESS when $A = 0.3$, $d_p = 30$ nm

6 Conclusion

In this paper, unsteady problem of solidification in a LHTES based on NEPCM is studied by means of FEM. Various shapes of inner cylinder, size of nanoparticles and

CuO-water volume fraction are utilized to investigate the solidification process. Results reveal that using nanoparticles can accelerate the discharging rate. Using higher amplitude leads to expedite the solidification rate. A , N and ϕ have direct relationship with solidification rate.

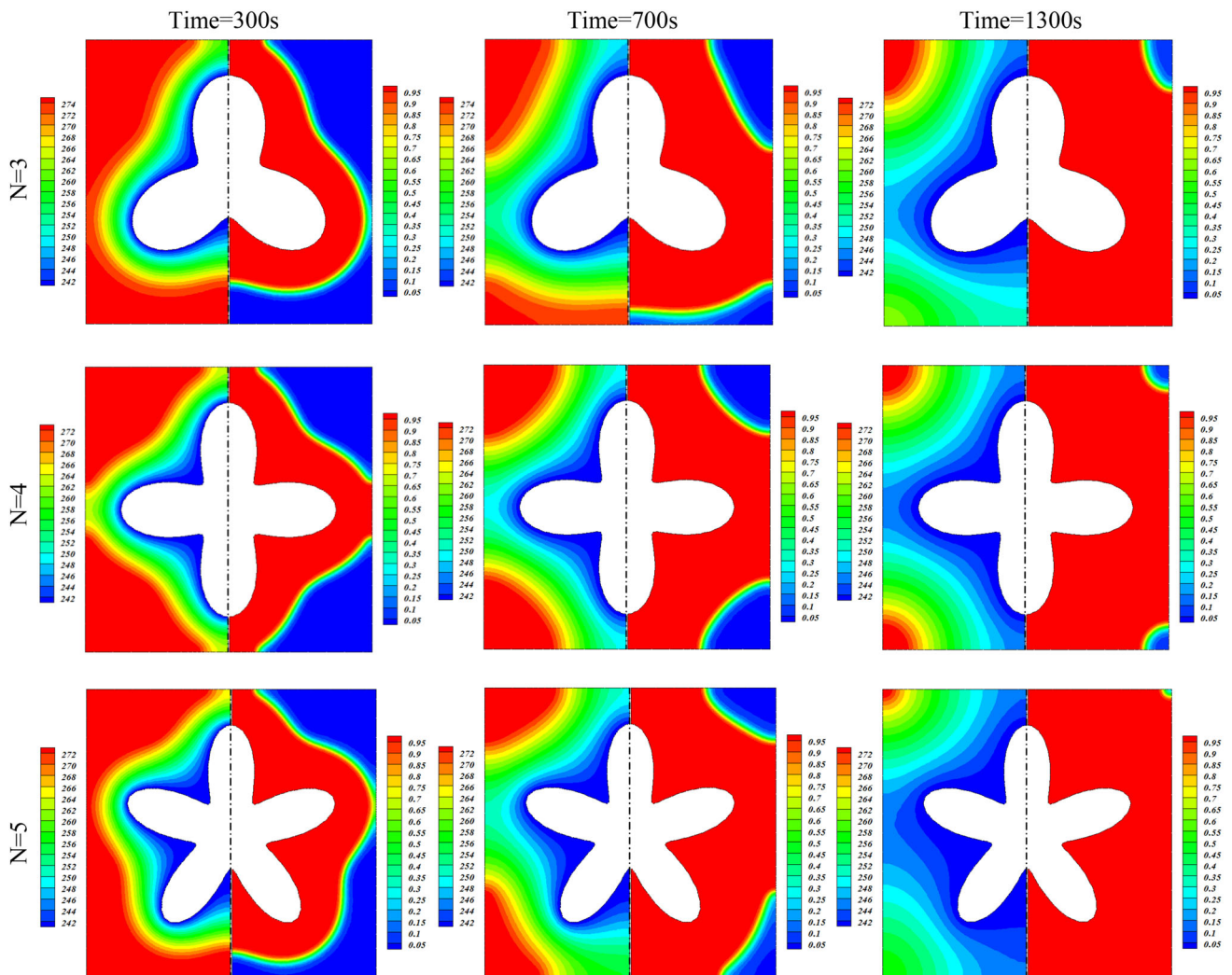


Fig. 7 Solid fraction (right side) and temperature (left side) contour plots at three different time steps during solidification process of LHTSS when $A = 0.5$, $d_p = 30$ nm

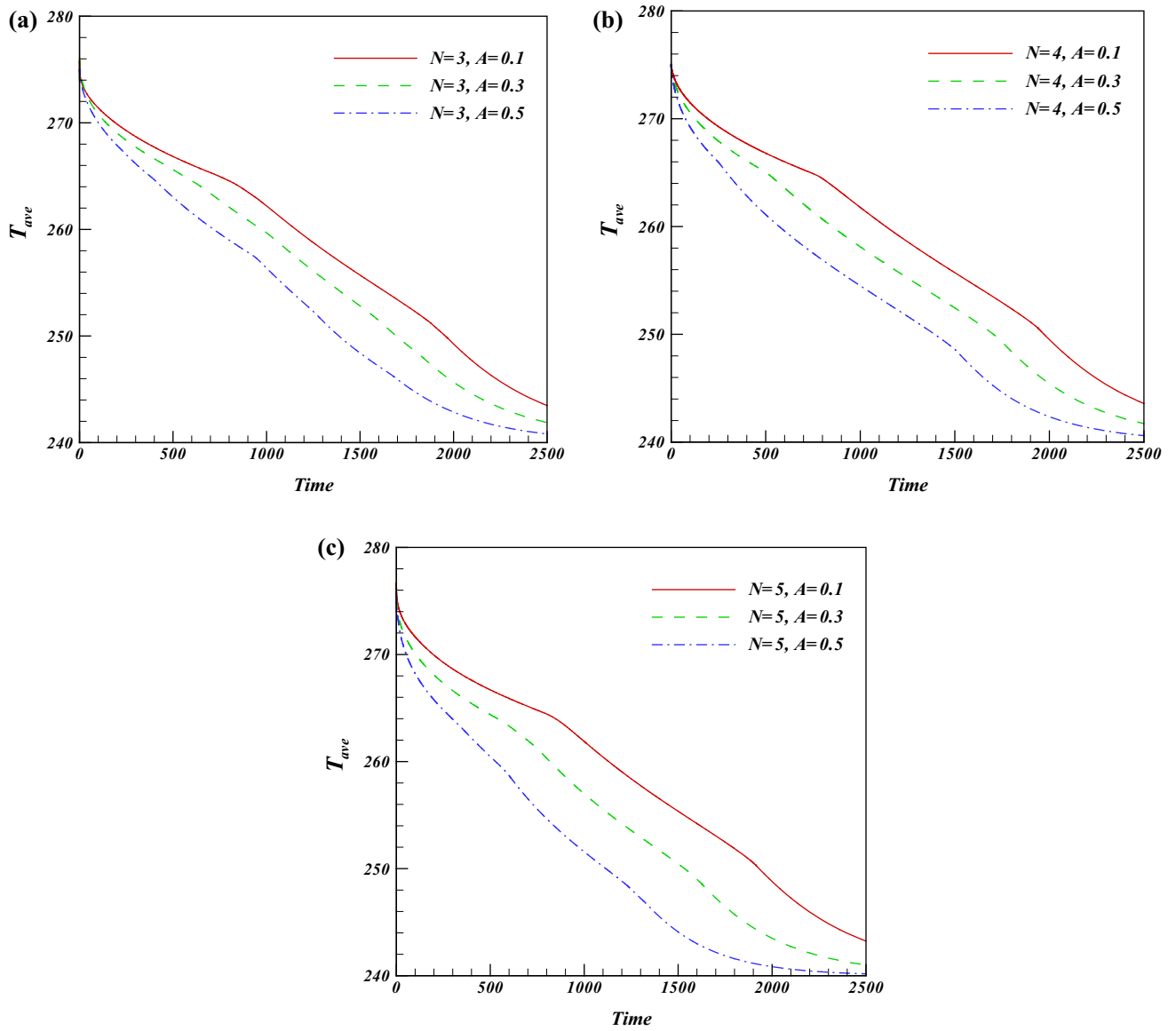


Fig. 8 Effects of A , N on average temperature variations over computational domain during solidification process when $\phi = 0.04$, $d_p = 30$ nm

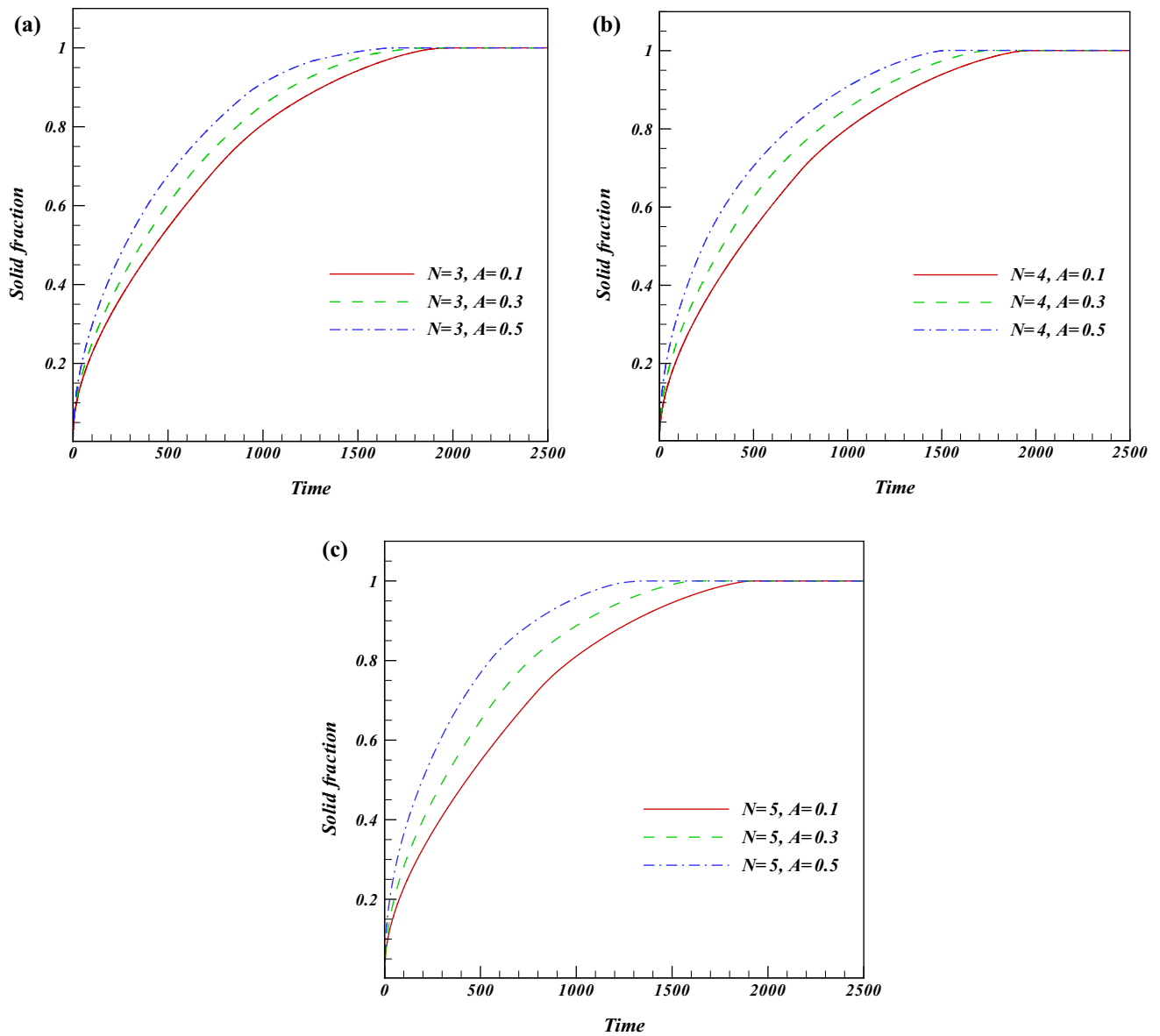


Fig. 9 Effects of A , N on solid fraction during solidification process when $\phi = 0.04$, $d_p = 30$ nm

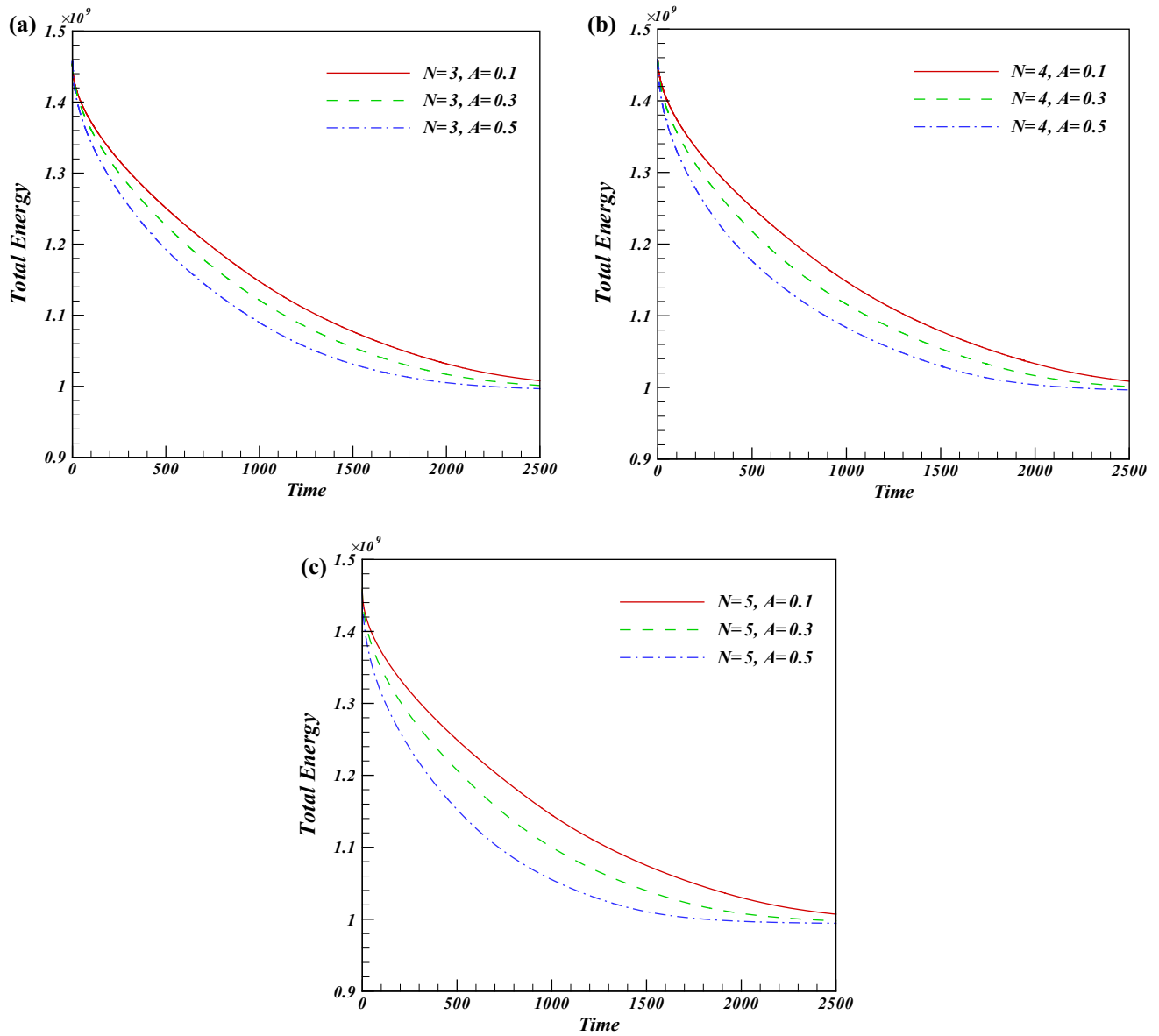
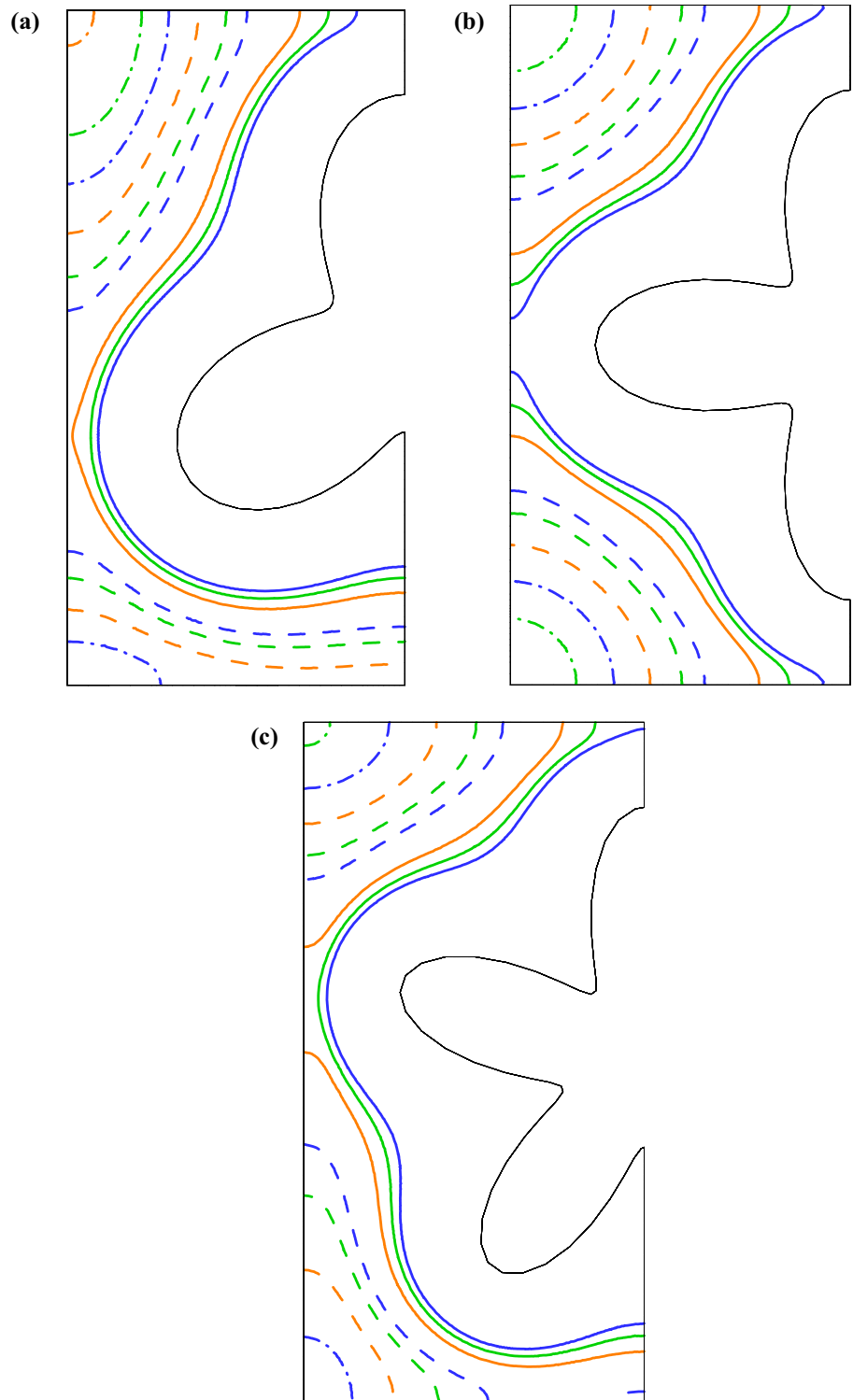


Fig. 10 Effects of A , N on total energy released during the discharging process in LHTESS when $\phi = 0.04$, $d_p = 30$ nm

Fig. 11 Effect of diameter of nanoparticles on Phase change front [green ($d_p = 30$ nm), orange ($d_p = 40$ nm), blue ($d_p = 50$ nm)] at various times (time = 300 s (solid line), time = 700 s (broken line), time = 1300 s (dotted broken line)] when $A = 0.5$, $\phi = 0.04$ (color figure online)



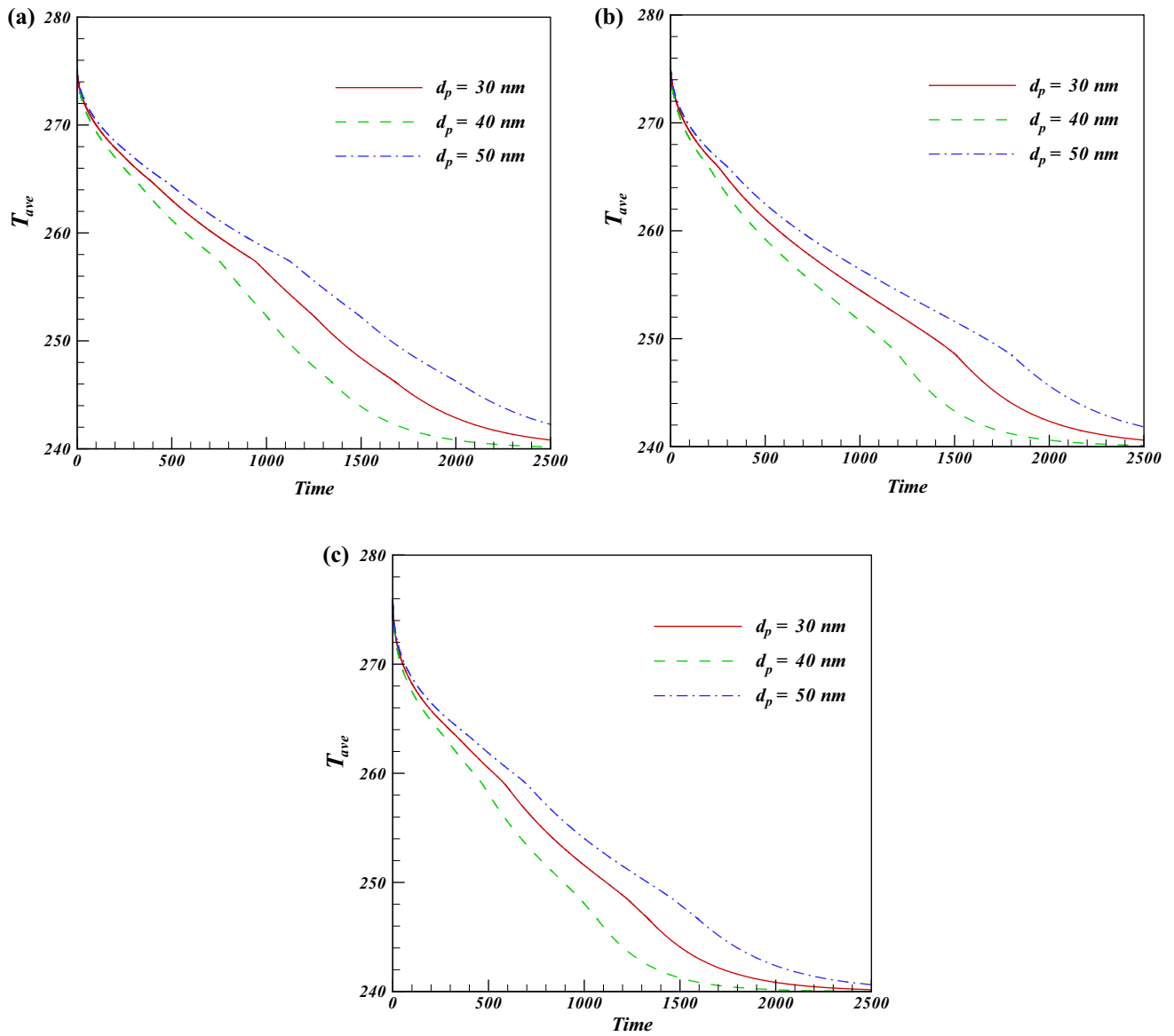


Fig. 12 Effects of d_p , N on average temperature variations over computational domain during solidification process when $\phi = 0.04$, $A = 0.5$

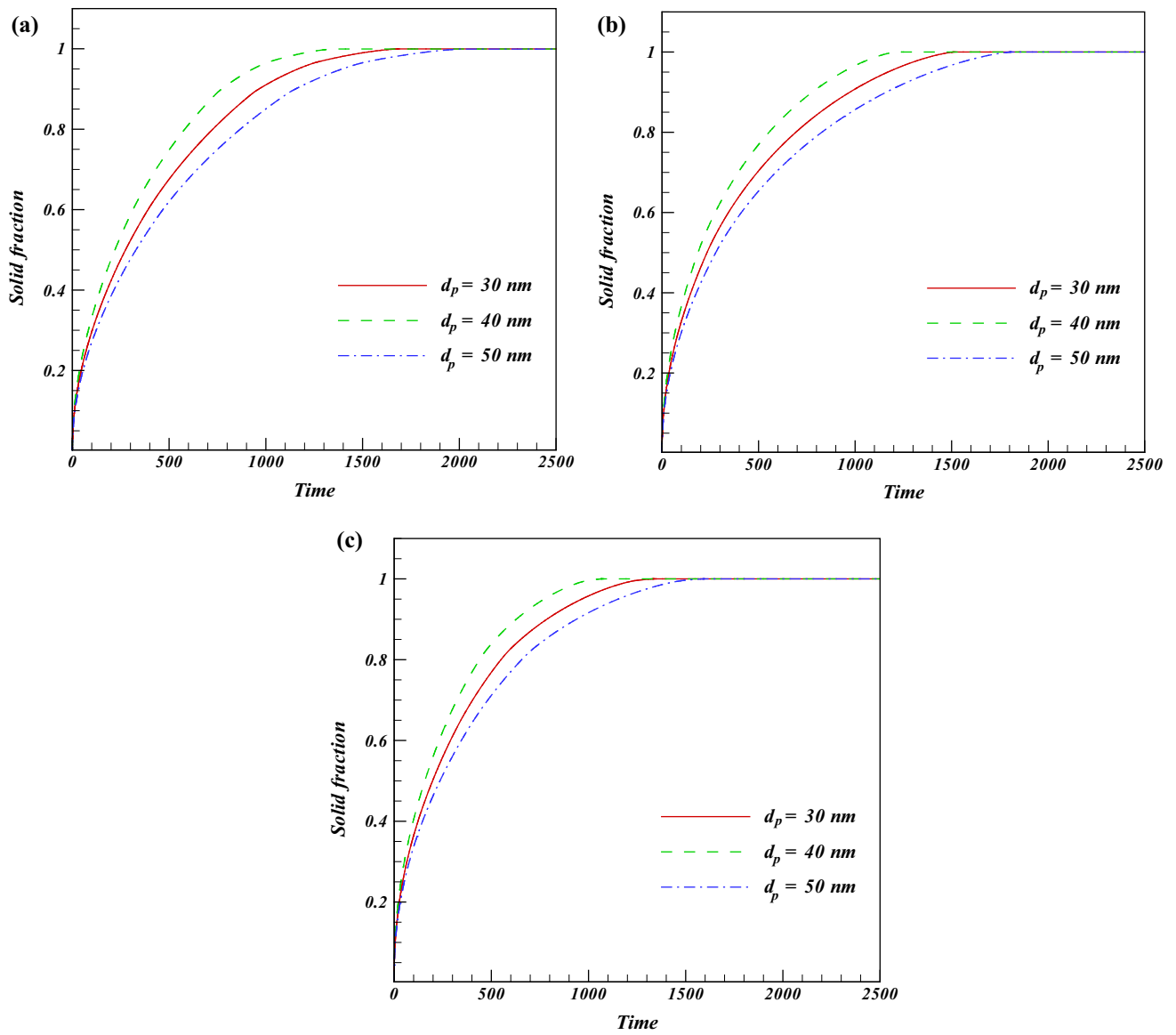


Fig. 13 Effects of d_p , N on solid fraction during solidification process when $\phi = 0.04$, $A = 0.5$

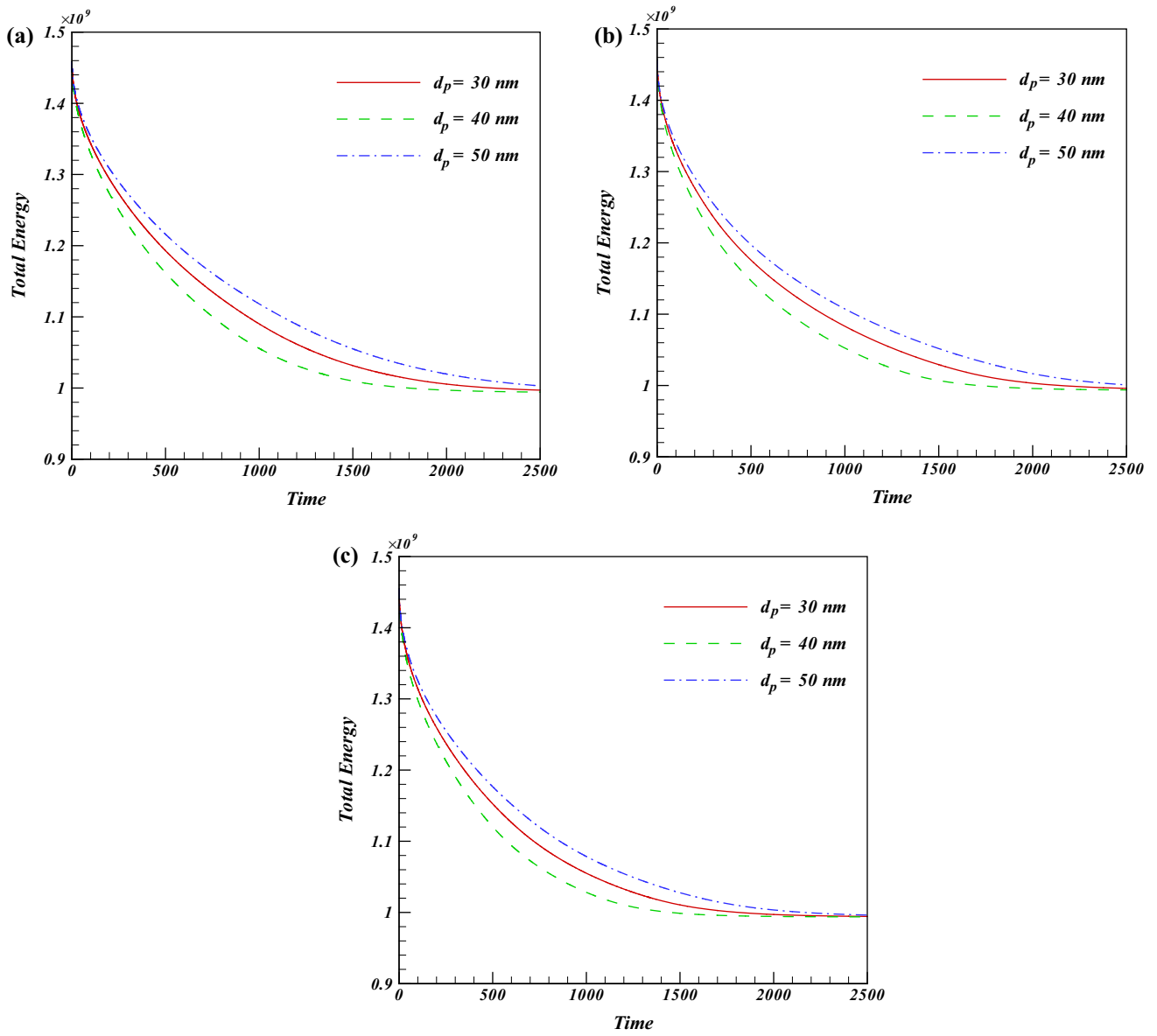
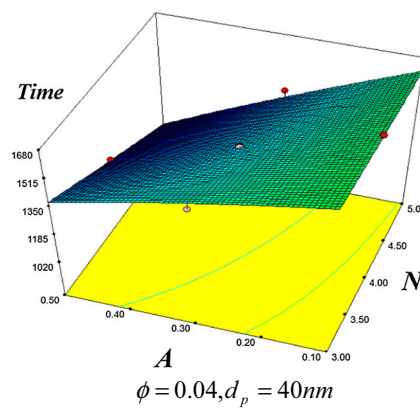
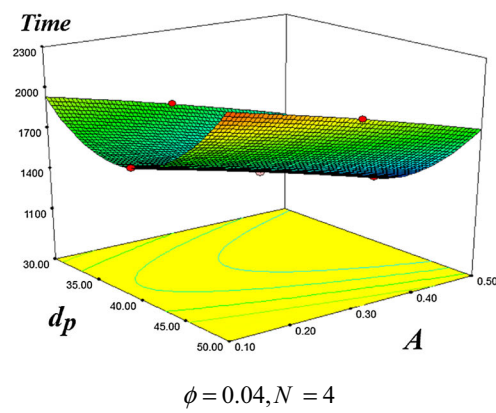
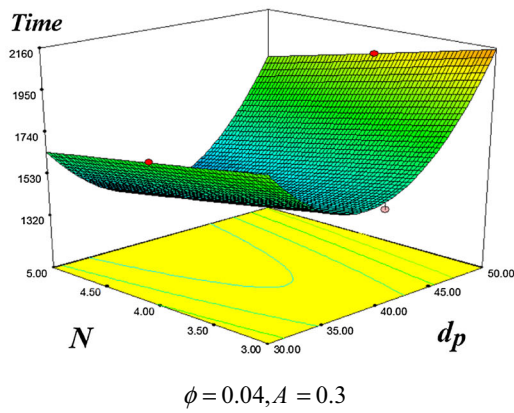
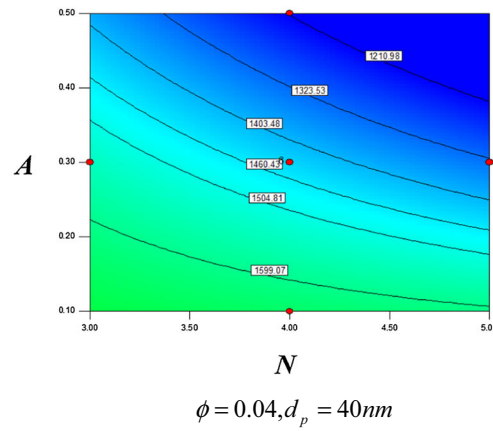
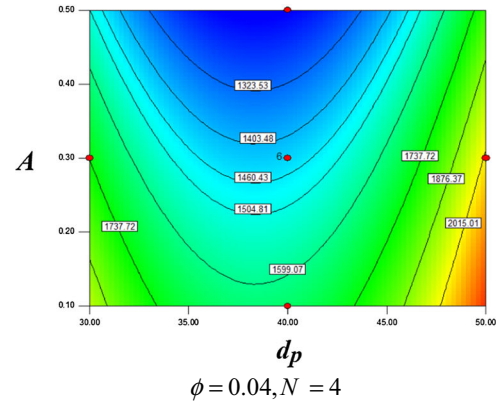
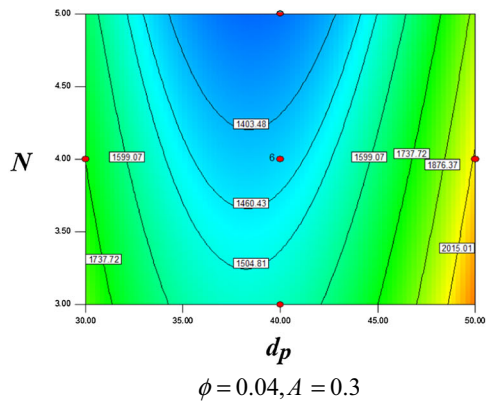


Fig. 14 Effects of d_p , N on total energy released during the discharging process in LHTESS when $\phi = 0.04$, $A = 0.5$



◀ **Fig. 15** Full solidification time for different values A , N , d_p

Acknowledgements This paper has been supported by the National Sciences Foundation of China (NSFC) (No. U1610109), Yingcai Project of CUMT (YC2017001), PAPD and UOW Vice-Chancellor's Postdoctoral Research Fellowship.

References

- Abro KA, Khan I (2017) Analysis of the heat and mass transfer in the MHD flow of a generalized Casson fluid in a porous space via non-integer order derivatives without a singular kernel. *Chin J Phys* 55:1583–1595
- Ahmad R, Mustafa M (2016) Model and comparative study for rotating flow of nanofluids due to convectively heated exponentially stretching sheet. *J Mol Liq* 220:635–641
- Ahmed N, Khan U, Mohyud-Din ST (2017) Unsteady radiative flow of chemically reacting fluid over a convectively heated stretchable surface with cross-diffusion gradients. *Int J Thermal Sci* 121:182–191
- Chamkha AJ, Ahmed SE, Aloraier AS (2010) Melting and radiation effects on mixed convection from a vertical surface embedded in a non-Newtonian fluid saturated non-Darcy porous medium for aiding and opposing flows. *Int J Phys Sci* 5:1212–1224
- Darzi AAR, Jourabian M, Farhadi M (2016) Melting and solidification of PCM enhanced by radial conductive fins and nanoparticles in cylindrical annulus. *Energy Convers Manag* 118:253–263
- Ellahi R, Hassan M, Zeeshan A, Khan AA (2016) The shape effects of nanoparticles suspended in HFE-7100 over wedge with entropy generation and mixed convection. *Appl Nanosci* 6:641–651
- Garooi F, Hoseininejad F, Rashidi MM (2016) Numerical study of heat transfer performance of nanofluids in a heat exchanger. *Appl Therm Eng* 105:436–455
- Haq RU, Kazmi SN, Mekkaoui T (2017a) Thermal management of water based SWCNTs enclosed in a partially heated trapezoidal cavity via FEM. *Int J Heat Mass Transf* 112:972–982
- Haq RU, Shahzad F, Al-Mdallal QM (2017b) MHD pulsatile flow of engine oil based carbon nanotubes between two concentric cylinders. *Results Phys* 7:57–68
- Hassan GE, Youssef ME, Mohamed ZE, Ali MA, Hanafy AA (2016) New temperature-based models for predicting global solar radiation. *Appl Energy* 179:437–450
- Hayat T, Qayyum S, Imtiaz M, Alsaedi A (2016a) Comparative study of silver and copper water nanofluids with mixed convection and nonlinear thermal radiation. *Int J Heat Mass Transf* 102:723–732
- Hayat T, Nisar Z, Yasmin H, Alsaedi A (2016b) Peristaltic transport of nanofluid in a compliant wall channel with convective conditions and thermal radiation. *J Mol Liq* 220:448–453
- Hayat T, Muhammad T, Shehzad SA, Alsaedi A (2017) On magnetohydrodynamic flow of nanofluid due to a rotating disk with slip effect: a numerical study. *Comput Methods Appl Mech Eng* 315:467–477
- Ismail K, Alves C, Modesto M (2001) Numerical and experimental study on the solidification of PCM around a vertical axially finned isothermal cylinder. *Appl Therm Eng* 21:53–77
- Li J, Liu L, Zheng L, Bin-Mohsin B (2016) Unsteady MHD flow and radiation heat transfer of nanofluid in a finite thin film with heat generation and thermophoresis. *J Taiwan Inst Chem Eng* 67:226–234
- Mushtaq A, Mustafa M, Hayat T, Alsaedi A (2014) Nonlinear radiative heat transfer in the flow of nanofluid due to solar energy: a numerical study. *J Taiwan Inst Chem Eng* 45:1176–1183
- Raju CSK, Sandeep N, Sugunamma V (2016) Unsteady magneto-nanofluid flow caused by a rotating cone with temperature dependent viscosity: a surgical implant application. *J Mol Liq* 222:1183–1191
- Shahzad N, Zeeshan A, Ellahi R, Vafai K (2016) Convective heat transfer of nanofluid in a wavy channel: Buongiorno's mathematical model. *J Mol Liq* 222:446–455
- Sheikholeslami M (2018) Numerical simulation for solidification in a LHTESS by means of nano-enhanced PCM. *J Taiwan Inst Chem Eng* 86:25–41
- Sheikholeslami M, Chamkha AJ (2016) Electrohydrodynamic free convection heat transfer of a nanofluid in a semi-annulus enclosure with a sinusoidal wall. *Numer Heat Transf Part A* 69:781–793
- Sheikholeslami M, Ellahi R (2015) Three dimensional mesoscopic simulation of magnetic field effect on natural convection of nanofluid. *Int J Heat Mass Transf* 89:799–808
- Sheikholeslami M, Ganji DD (2016) Nanofluid convective heat transfer using semi analytical and numerical approaches: a review. *J Taiwan Inst Chem Eng* 65:43–77
- Sheikholeslami M, Rokni HB (2017) Simulation of nanofluid heat transfer in presence of magnetic field: a review. *Int J Heat Mass Transf* 115:1203–1233
- Sheikholeslami M, Li Z, Shafee A (2018a) Lorentz forces effect on NEPCM heat transfer during solidification in a porous energy storage system. *Int J Heat Mass Transfer* 127:665–674
- Sheikholeslami M, Shehzad SA, Li Z (2018b) Water based nanofluid free convection heat transfer in a three dimensional porous cavity with hot sphere obstacle in existence of Lorenz forces. *Int J Heat Mass Transfer* 125:375–386
- Sobamowo MG (2016) Nonlinear vibration analysis of single-walled carbon nanotube conveying fluid with slip boundary conditions using variational iterative method. *J Appl Comput Mech* 2:208–221
- Tao YB, He YL (2015) Effects of natural convection on latent heat storage performance of salt in a horizontal concentric tube. *Appl Energy* 143:38–46

Publisher's Note Springer Nature remains neutral with regard to jurisdictional claims in published maps and institutional affiliations.